NANO LETTERS

pubs.acs.org/NanoLett

Letter

Gate-Tunable Resonance State and Screening Effects for Proton-Like Atomic Charge in Graphene

Mykola Telychko, Keian Noori, Hillol Biswas, Dikshant Dulal, Zhaolong Chen, Pin Lyu, Jing Li, Hsin-Zon Tsai, Hanyan Fang, Zhizhan Qiu, Zhun Wai Yap, Kenji Watanabe, Takashi Taniguchi, Jing Wu, Kian Ping Loh, Michael F. Crommie, Aleksandr Rodin,* and Jiong Lu*

Cite This: *Nano Lett.* 2022, 22, 8422–8429

Read Online

ACCESS | Metrics & More | Article Recommendations | Supporting Information

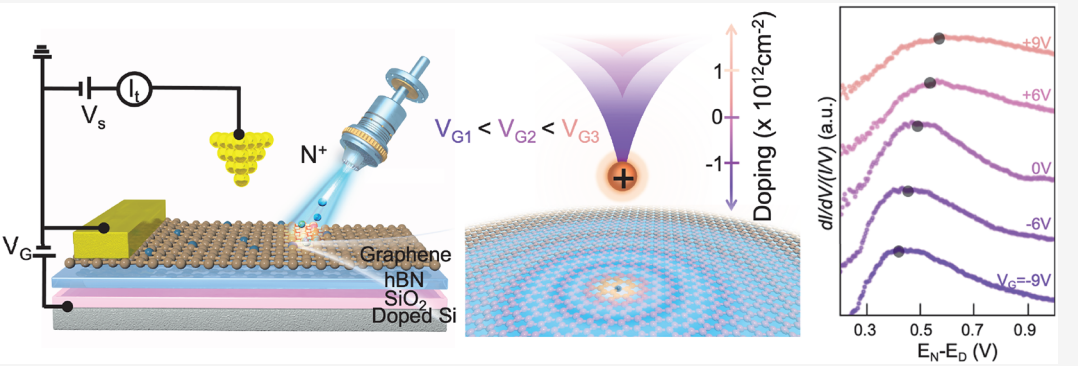

ABSTRACT: The ability to create a robust and well-defined artificial atomic charge in graphene and understand its carrier-dependent electronic properties represents an important goal toward the development of graphene-based quantum devices. Herein, we devise a new pathway toward the atomically precise embodiment of point charges into a graphene lattice by posterior (N) ion implantation into a back-gated graphene device. The N dopant behaves as an in-plane proton-like charge manifested by formation of the characteristic resonance state in the conduction band. Scanning tunneling spectroscopy measurements at varied charge carrier densities reveal a giant energetic renormalization of the resonance state up to 220 meV with respect to the Dirac point, accompanied by the observation of gate-tunable long-range screening effects close to individual N dopants. Joint density functional theory and tight-binding calculations with modified perturbation potential corroborate experimental findings and highlight the short-range character of N-induced perturbation.

KEYWORDS: *graphene, nitrogen doping, impurity, back-gated device, ion implantation*

The relativistic-like electronic dispersion in graphene offers a rich platform for studying exotic quantum electrodynamics phenomena in a condensed-matter setup as well as for developing novel electronics and quantum optics.[1,2] This photon-like band structure also makes graphene electrons much less amenable to electrostatic confinement compared to conventional materials. The ability to create a robust atomically precise Coulomb charge in graphene and understand its carrier-dependent electronic properties at the nanoscale represents an important goal toward the development of graphene-based quantum devices. To date, the Coulomb charge problem in graphene has been addressed via scanning tunneling microscopy (STM)-assisted studies of highly charged transition-metal adatoms,[3−7] one-dimensional molecular arrays on graphene,[8,9] and creating a vacancy in the back-gated graphene device.[10] Nevertheless, the extent of the potential produced by "out-of-plane" charge centers above graphene is expected to be very different from the "in-plane" charges hosted in graphene,[11−13] while in-plane carbon vacancies tend to undergo structural reconstructions manifested by emergence of characteristic spin-polarized states.[14] This distinction hinges on a question: Is it possible to controllably fabricate in-plane point positive charges in a graphene lattice in a *true* two-dimensional (2D) limit and further probe the associated response of the Dirac Fermions as a function of carrier density?

The ideal scenario of an in-plane Coulomb charge center assumes a point charge residing in the graphene plane without imposing any lattice deformations. The most viable way to

Received: June 3, 2022
Revised: October 5, 2022
Published: October 10, 2022

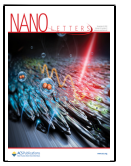

https://doi.org/10.1021/acs.nanolett.2c02235
Nano Lett. 2022, 22, 8422–8429

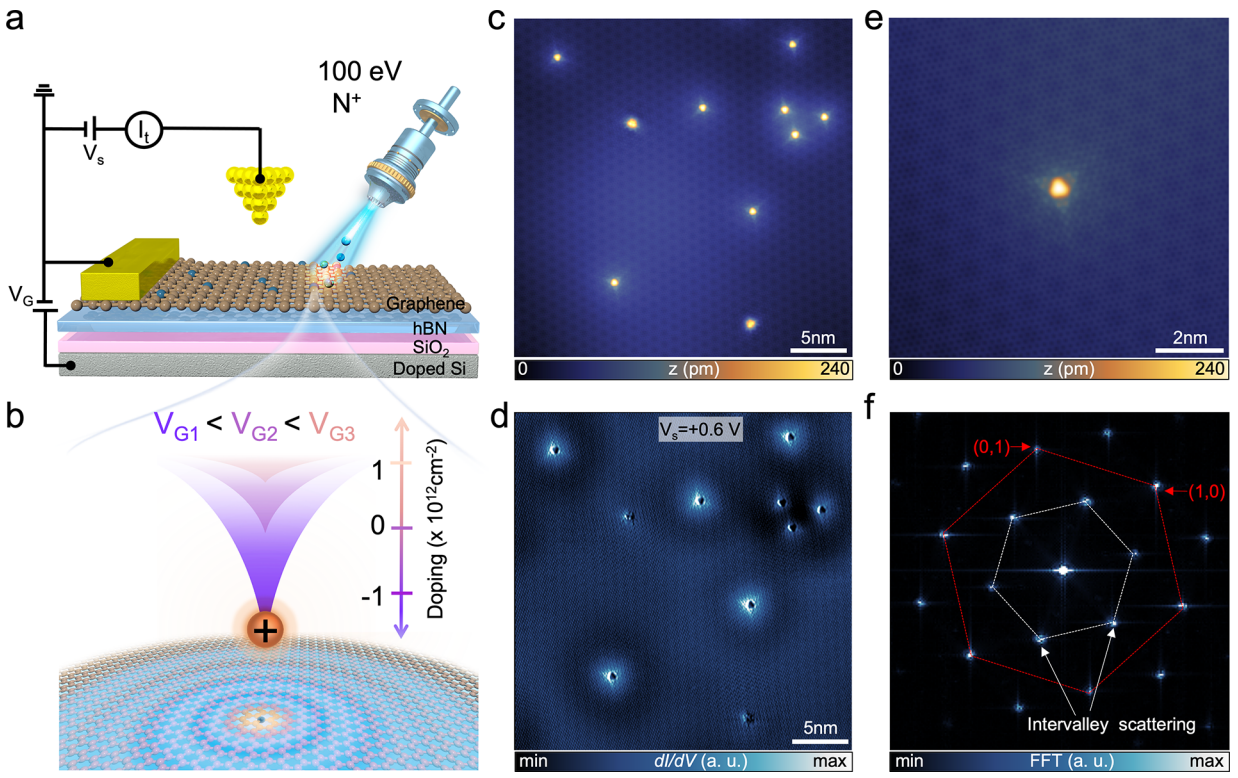

Figure 1. Creating substitutional nitrogen dopants in back-gated G/BN. (a) Schematics showing the route toward incorporation of N dopant into back-gated G/BN using low-energy (+100 eV) N^+ ion implantation. (b) Schematic illustration of a tunable proton-induced potential via gating. (c) Large-scale STM image reveals the presence of individual substitutional N atoms. (d) dI/dV map acquired at V_s = +0.6 V over the same surface area as STM image in panel (c). (e) Enlarged image of individual N dopant. (f) Fast Fourier transformation of the STM image of individual N dopant.

create such a scenario is to utilize nitrogen (N) substitution into graphene. The similarity of atomic radii of N and C, accompanied by the ability of N to adopt sp^2 hybridization, allows for its facile incorporation into the graphene lattice. In addition, due to the proximity of N and C in the periodic table and one more proton of N nuclei than C, sp^2-like N substitution in graphene is essentially equivalent to injecting a single proton into one of the lattice sites of pristine graphene. Previously both atom-resolved imaging[15−24] and sample-averaged spectroscopic techniques[25−29] have been extensively deployed to probe structural and electronic properties of N impurities in graphene. Nevertheless, all these studies utilized heavily doped graphene layers with altered intrinsic electronic structure due to the presence of the underlying substrates, including silicon carbide,[15,22,30] Cu(111),[20,23] or another graphene layer,[24] that obstructed deciphering of both short- and long-range electronic effects associated with N atoms in pristine single-layer graphene at varied charge carrier densities. Therefore, back-gated graphene-boron nitride (G/BN) devices harboring atomically smooth and charge-homogeneous interfaces[31] may provide an ideal platform to probe unique electronic behavior around N impurities in a tunable and poorly screened environment. On the other hand, the viable routes of high-yield posterior sp^2-like N incorporation directly into back-gated graphene device have been hitherto missing.

Here, we have devised a well-controlled N^+ ion implantation routine allowing for a high-yield sp^2-like incorporation of individual N atoms into the graphene lattice (Figure 1a,b) in a back-gated G/BN device. Individual N dopants behave as in-plane artificial protons, manifested by the emergence of a broad resonance state (E_N) above the Dirac point together with long-range Friedel oscillations in the vicinity of N dopants. Using gate-tunable dI/dV measurements, we demonstrate that the strength of the proton's potential can be effectively modified via tuning charge carrier density in graphene, leading to a giant gate-tunable energetic shift of the N-induced resonance state (E_N) with respect to the Dirac point. Such a phenomenon not only has not been demonstrated to date but also is in stark contrast to gate-tunable behavior of other reported atomically precise impurities in graphene with electronic resonances pinned to the Dirac point. Density functional theory (DFT) and effective tight-binding (TB) theory calculations with modified on-site perturbation potential and hopping constant corroborate the emergence of the new resonance state and its associated gate-tunable correlation effects.

We first fabricated the back-gated device consisting of chemical vapor deposition (CVD)-grown monolayer graphene on top of a hexagonal boron-nitride flake (G/BN) placed onto a SiO_2 substrate, as shown in Figure 1a (also see Supporting Information). Gate voltage (V_G), applied between the electrostatically grounded graphene sheet and the doped Si wafer, enables the tunability of the carrier density in graphene (Figure 1b).

Our route toward the N atoms embodiment in back-gated G/BN (Figure 1a) relies on its posterior bombardment using low-energy (+100 eV) N^+ ions in ultrahigh vacuum conditions, as illustrated in Figure 1a (see Methods for further details). This process results in a robust sp^2-like incorporation of individual N atoms into graphene. The representative STM

https://doi.org/10.1021/acs.nanolett.2c02235
Nano Lett. 2022, 22, 8422−8429

images reveal that the surface of the G/BN after N^+ implantation is decorated with abundant triangular-shaped features attributed to the individual N dopants (Figure 1c). It is noted that the apparent height of the in-plane N sites strongly depends on applied bias voltage (see Figure S3). A higher apparent height observed in a larger positive sample bias is attributed to their enhanced empty density of electronic states as discussed in detail further below.

High-resolution STM imaging (Figure 1e) and dI/dV mapping (Figure 1d) of the single N dopant in graphene demonstrate the characteristic $\sqrt{3} \times \sqrt{3}$ pattern associated with the intervalley electron scattering processes, which has also been revealed in the vicinity of atomic-scale defects, including hydrogen adatoms[32] and carbon vacancies.[10,33] Characteristic spots attributed to electron backscattering processes between K and K′ valleys are also evident in the Fourier-transformed STM image (Figure 1f).

Next, we probed the electronic properties of the N dopants via the acquisition of the site-specific dI/dV point spectra in the nearly neutral doping regime (i.e., V_G = 0 V), which reveal several prominent features (Figure 2a,b). These include (i) a gap-like feature (∼130 meV) centered at the Fermi level (E_F) attributed to the phonon-assisted inelastic tunneling[34] and (ii) an electron−hole asymmetry with reduced (increased) spectral weight of the hole (electron) dI/dV branch, decaying with distance from the N site (Figure 3a). This indicates a net positive charge of the N dopant[19,35] as expected from a partially screened proton in the graphene lattice. (iii) The dI/dV spectra acquired over the N site (Figure 2a) and in its proximity reveal a broad resonance state (denoted as E_N) centered at ∼590 meV above E_F, as further illustrated by the normalized dI/dV spectra (see Supporting Information). The 2D contour map of the dI/dV spectra (Figure 2b) reveals the spatial extent of the N-induced resonance state gradually decaying with distance from the N site and fading beyond ∼1.7 nm.

In addition, bias-dependent dI/dV maps reveal characteristic concentric rings in the vicinity of the N dopant that are attributed to the Friedel oscillations (FOs). The dI/dV maps acquired at negative sample biases (Figure 2c) display an attenuated dI/dV intensity in direct proximity to the N site surrounded by brighter FO rings. In contrast, dI/dV maps acquired at positive sample biases (Figure 2d) feature a reversed contrast with an enhanced dI/dV signal close to the N site, surrounded by FO rings with a lower dI/dV intensity. It is noteworthy that the diameter of the FO rings scales inversely with the bias voltage as revealed also by dI/dV line scans normalized with respect to the tunneling conductance value (i.e., dI/dV/(I/V)), acquired at different V_s values shown in Supporting Information. For instance, the dI/dV line scans acquired at V_s = −0.6, −0.5, and −0.4 V feature FO rings with a diameter of 4.16, 5.76, and 7.30 nm, respectively. The FO diameter is also found to be tunable by charge-carrier density as evidenced by dI/dV line scans acquired at varied V_G (see Supporting Information).

We then explored carrier-dependent electronic properties of the N dopant by acquiring the dI/dV spectra at various V_G values ranging from V_G = −9 V (p-doped regime) to V_G = +9 V (n-doped regime). Prior to this, gate-dependent dI/dV spectra acquired over nearby graphene (>10 nm away) exhibit a characteristic energy shift of Dirac point ("dip-feature" marked by red dots) in Figure 4b, whereby the carrier concentration at V_G = +9 V is estimated to be $n_e \approx 1.8 \times 10^{12}$ cm^{-2} using a standard capacitor model[36,37] (see Methods). Note that the charge neutrality point of graphene is close to V_G = 0 (see Supporting Information). In contrast, the normalized point dI/dV spectra (see Supporting Information) acquired over the N site reveal a slightly V_G-dependent energetic shift of E_N, from 497 mV (at V_G = −9 V) to 464 mV (at V_G = 0 V) (Figure 4a). Further, gating graphene into the n-doped regime (V_G = +9 V) leads to a notable broadening of E_N and an attenuation of its spectral weight.

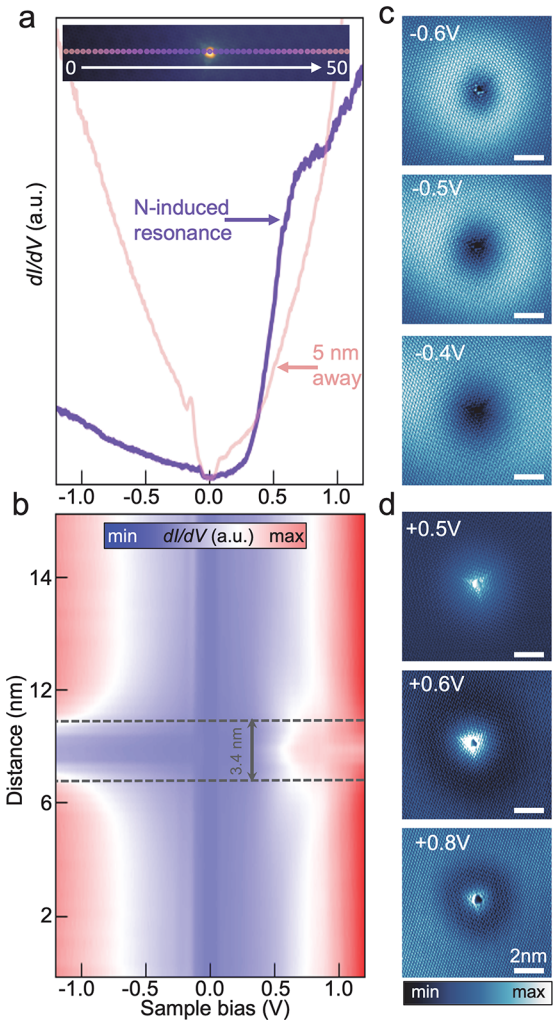

Figure 2. Characterization of individual N dopants. (a) dI/dV spectra acquired over N-site and pristine graphene. (b) 2D color-coded contour plot constructed from the set of point dI/dV spectra acquired along the line traversing single N dopant indicated in the inset STM image in panel (a). (c, d) dI/dV maps acquired at negative (c) and positive (d) bias voltages indicated in top-left corners. Length of each scale bar is 2 nm. The dI/dV spectra were acquired at tunneling set point V_s = +1.2 V, I = 2 nA.

The site-specific dI/dV measurements discussed above enable the determination of the V_G-dependent energetic position of the E_N with respect to the Dirac point (Figure 4c). With account of the phonon-assisted inelastic tunneling process[34] (details in Methods), it is evident that a gradual variation of the back-gate voltage V_G from −9 to +9 V leads to a monotonic shift of E_N from ∼415 to ∼635 mV relative to the Dirac point (black dots in Figure 4c). Such a giant carrier density-dependent energetic renormalization of the N-induced resonance state with respect to the Dirac point (i.e., ∼220

https://doi.org/10.1021/acs.nanolett.2c02235
Nano Lett. 2022, 22, 8422−8429

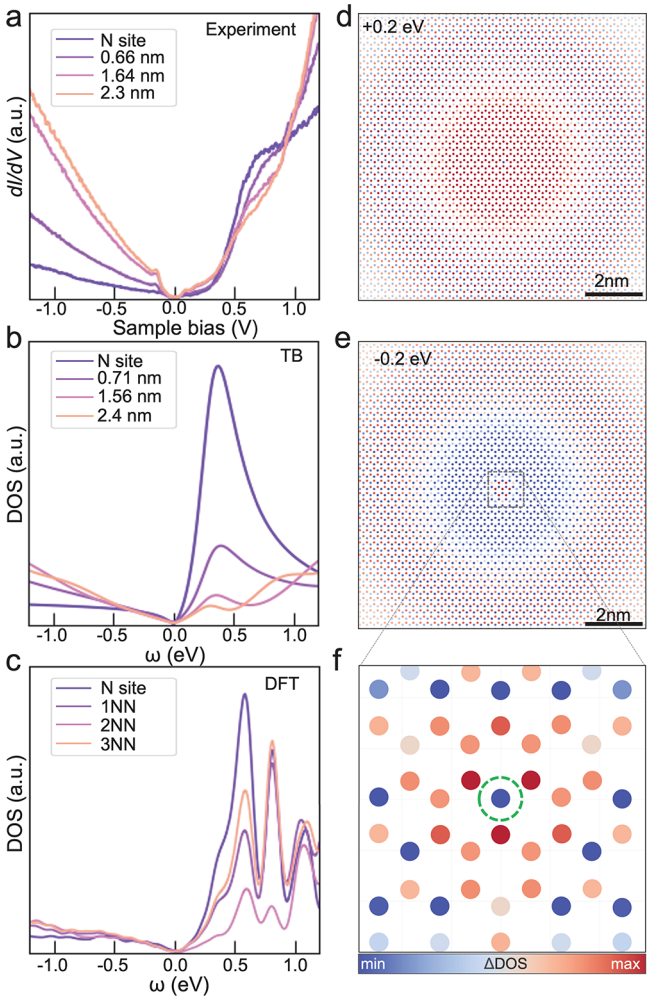

Figure 3. Electronic structures of individual N dopants. (a) dI/dV spectra acquired over an N site and its vicinity (tunneling set point V_s = +1.2 V, I = 2 nA). (b) Site-specific DOS spectra acquired over an N site and its vicinity using TB model for perturbation potential (Δ) values of: $\Delta_0 = -7$ eV, $\Delta_1 = -0.7$ eV, and $\delta t = 0.5$ eV. (c) DFT-calculated DOS of the N site and its first (1NN), second (2NN), and third (3NN) nearest C neighbors in a 10 × 10 supercell. (b, c) ω is the energy measured from the Dirac point. (d, e) Real space spectral function maps calculated at energies of +0.2 (d) and −0.2 (e) eV using TB formalism. The colors represent the local deviation of the spectral function from the value of pristine graphene (ΔDOS). (f) Enlarged image of area marked by square in panel (e). Dashed green circle marks the position of N site.

meV) sets N dopants apart from other previously studied impurities residing in a back-gated graphene. Specifically, it has been shown that the electronic resonance states associated with hydrogen adatoms,[18,38] single carbon vacancies, and[10] cobalt clusters[4] are energetically pinned to the Dirac point and thus exhibit a rigid shift with the Dirac point as a function of V_G. The nonrigid shift of molecular frontier orbitals with respect to V_G has been recently attributed to many-electron interactions and gate-tunable graphene's polarization effects.[39] In the most general sense, the peak in the spectral function can be viewed as a consequence of the attractive potential created by the extra proton in the nitrogen nucleus. The electronic density in the material and the associated screening effects can be controlled by gating. Modifying the screening alters the potential produced by the proton, consequently shifting the peak in the spectral function.

We first carried out DFT calculations to understand both local structural and electronic properties of a single N dopant in graphene. Specifically, DFT-calculated projected density of states (DOS) for the p_z orbitals of the N dopant, along with its first, second, and third nearest C neighbors, reveals a peak centered at ∼500 meV above E_F (Figure 3c), consistent with the experimental spectrum. The presence of multiple peaks above the Fermi energy in the DFT spectra arises from an artifact of N-impurity interactions caused by the periodic boundary conditions[40] imposed by the finite supercell size. In the limit of an infinitely large cell, as in the present TB formulation, these peaks would vanish. We would like to point out that the salient features of the DFT spectra, namely, the location of the N-induced peak and its weakening away from a N site, are qualitatively in agreement with our experimental observations presented in Figure 3a. Importantly, our DFT calculations also indicate that the presence of N in graphene renders a rather negligible lattice distortion, with almost identical lengths of C−N (1.41 Å) and C−C (1.42 Å) bonds. Moreover, graphene's lattice remains flat, retaining its sp^2 hybridization, preventing any spin-flip processes, and preserving the separation of graphene π and σ bands. Consequently, N substitution allows for the formation of the desired in-plane Coulomb center while maintaining the sp^2 integrity of graphene.

To describe the effects of the N dopant, we employ tight-binding calculations with the formalism described in ref 41 using a Julia language[42] package.[43] Since the TB approach with nearest-neighbor hopping works well for graphene, and since the p_z orbitals of nitrogen are smaller than those of carbon (see Supporting Information), it should be possible to only change the on-site energy of the dopant and its neighbors (by adding energies Δ_0 and Δ_1, respectively) and adjust the hopping parameters (δt) to describe the N-induced broad resonance state. Indeed, we find that such a perturbation, with $\Delta_0 = -7$ eV, $\Delta_1 = -0.7$ eV, and $\delta t = 0.5$ eV, shown in Figure 3b, gives a good agreement with the ab initio results (Figure 3c), reinforcing the short-range nature of the N-induced perturbation. In addition, real-space spectral function maps calculated using the TB formalism reproduce experimental dI/dV maps by revealing both the characteristic triangular shape near to N (Figure 3f) and the surrounding FO concentric rings, arising from the intravalley scattering[44] (Figure 3d,e). We note that earlier work[40] presents different TB parameters. We would like to emphasize that our values agree with the DFT profiles better and that both parametrizations capture the essential features and do not lead to different qualitative results.

As discussed above, substituting a C with an N can be viewed as injecting a proton into the system. Consequently, one might expect the emergence of long-range effects arising from the Coulomb potential produced by this proton instead of the short-range perturbation suggested by the DFT and TB calculations. To reconcile these two pictures, one can start with the proton-generated $1/r$ attractive potential, which gives rise to bound states with energies below the lowest kinetic energy that particles can have. In the case of graphene, the relevant system of particles corresponds to the π-band electrons. The DFT calculations confirm the existence of a deep energy bound state below the π band (Figure S8 and S9). Naturally, this state will become occupied, and the electron will screen

https://doi.org/10.1021/acs.nanolett.2c02235
Nano Lett. 2022, 22, 8422−8429

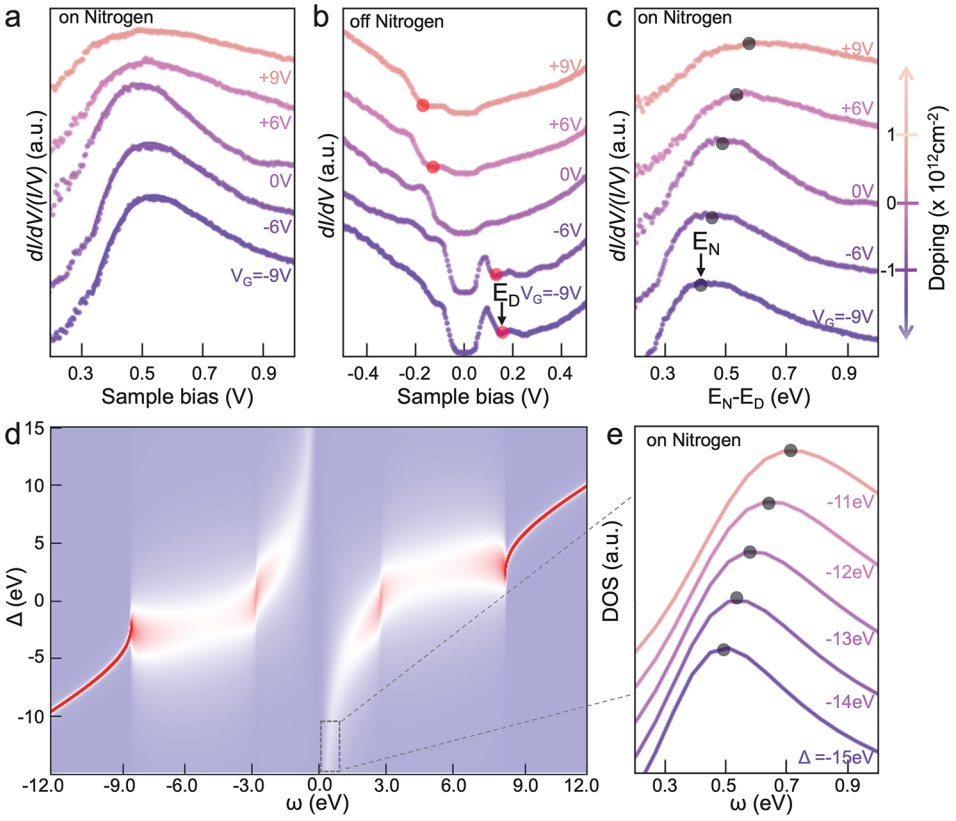

Figure 4. Gate-tunable electronic properties of N dopant. (a) Normalized dI/dV/(I/V) spectra acquired over N site at various V_G. (b) dI/dV spectra acquired over pristine graphene area at various V_G. Red dots mark positions of Dirac point (E_D). (c) Energetic positions of N-induced resonance state (E_N) with respect to E_D extracted from site-specific dI/dV spectra acquired at various V_G, with account of the phonon-assisted inelastic tunneling process. Black dots mark the maxima of E_N. (d) Color-coded TB spectral plot with $\omega = 0$ corresponding to the Dirac point. (e) TB spectra extracted for monotonously varied values of the perturbation potential (Δ). The dI/dV spectra were acquired at the tunneling set point of V_s = +1.2 V, I = 2 nA.

the proton, sharply diminishing the extent of the Coulomb potential. Additionally, the surrounding atoms also screen the positive charge, further reducing the potential's range.

One last question that remains is the gate-dependent renormalization of the N-induced resonance state (E_N) with respect to the Dirac point. A variation of carrier density in graphene is expected to further modulate the screened potential of the added proton, equivalent to tuning the on-site energy of the dopant and its neighbors, and the hopping parameter between them, in the TB formalism.

More specifically, sweeping the back-gate voltage from V_G = −9 V to V_G = +9 V, corresponding to an electron density of $n_e \approx 1.8 \times 10^{12}$ cm^{-2} in the system, provides additional screening to the already-screened proton, effectively weakening its ability to lower the potential energy of other electrons. In our toy model, this is equivalent to making on-site energies less negative and pushing the resonance state to higher energies (Figure 4d). While the entire band structure shifts to lower energy due to gating, the net effect is manifested as the V_G-dependent E_N resonance state lagging behind the Dirac point (Figure 4c). As the simplest illustration, we only include the on-site energy modification Δ for the nitrogen dopant and plot the dopant's spectral function for a range of Δ values in Figure 4d. The respective plots for the (next-)nearest carbon neighbor are shown in Supporting Information. We observe that, as the on-site potential is varied, the energy difference between the resonance in the conduction band and the Dirac point changes (Figure 4e), as seen in the experiment. In addition, one can expect the formation of a bound state below the band minimum for sufficiently large Δ values, as seen in Figure 4d.

In summary, we have devised a new route toward a controllable sp^2-like incorporation of N atoms into back-gated Gr/BN. The N dopant, seamlessly embedded into the graphene lattice, behaves as an artificial proton with dominant short-ranged potential perturbation, leading to the formation of a broad resonance state above the Dirac point. The strength of the proton's potential can be effectively modified via tuning charge carrier density in graphene, leading to a giant gate-tunable energetic renormalization of the resonance state up to 220 meV with respect to the Dirac point, which is is in a stark contrast to gate-tunable response of other atomically precise impurities in graphene reported to date. It can be envisaged that synergy of the uncovered atomically precise N$^+$ implantation technique, with a judiciously designed device patterning strategy, may enable facile fabrication of nanoscale linear[45,46] or circular[47−49] p−n junctions in graphene for developing novel electronics and quantum optics. In addition, controllable N substitution developed here may allow to trace the evolution of the gate-tunable bands associated with midgap states in Bernal-stacked bilayer graphene[24] and to address the Coulomb problem in the magic-angle twisted graphene bilayers with strong correlation effects.[50]

https://doi.org/10.1021/acs.nanolett.2c02235
Nano Lett. 2022, 22, 8422−8429

■ ASSOCIATED CONTENT

Supporting Information

The Supporting Information is available free of charge at https://pubs.acs.org/doi/10.1021/acs.nanolett.2c02235.

Experimental methods, including details of G/BN device fabrication and theoretical calculations; additional experimental dI/dV measurements, theoretical DOS and TB data (PDF)

■ AUTHOR INFORMATION

Corresponding Authors

Aleksandr Rodin − *Yale-NUS College, 138527, Singapore; Centre for Advanced 2D Materials, National University of Singapore, 117543, Singapore*; Email: aleksandr.rodin@yale-nus.edu.sg

Jiong Lu − *Department of Chemistry, National University of Singapore, 117543, Singapore; Centre for Advanced 2D Materials, National University of Singapore, 117543, Singapore; Institute for Functional Intelligent Materials, National University of Singapore, 117544, Singapore*; orcid.org/0000-0002-3690-8235; Email: chmluj@nus.edu.sg

Authors

Mykola Telychko − *Department of Chemistry, National University of Singapore, 117543, Singapore*; orcid.org/0000-0002-8156-8938

Keian Noori − *Institute for Functional Intelligent Materials, National University of Singapore, 117544, Singapore; Centre for Advanced 2D Materials, National University of Singapore, 117543, Singapore*

Hillol Biswas − *Department of Physics, National University of Singapore, 117542, Singapore; Centre for Advanced 2D Materials, National University of Singapore, 117543, Singapore*

Dikshant Dulal − *Yale-NUS College, 138527, Singapore*

Zhaolong Chen − *Institute for Functional Intelligent Materials, National University of Singapore, 117544, Singapore*

Pin Lyu − *Department of Chemistry, National University of Singapore, 117543, Singapore*

Jing Li − *Centre for Advanced 2D Materials, National University of Singapore, 117543, Singapore*

Hsin-Zon Tsai − *Department of Physics, University of California, Berkeley 94720 California, United States*

Hanyan Fang − *Department of Chemistry, National University of Singapore, 117543, Singapore*

Zhizhan Qiu − *Department of Chemistry, National University of Singapore, 117543, Singapore*

Zhun Wai Yap − *Yale-NUS College, 138527, Singapore*

Kenji Watanabe − *Research Center for Functional Materials, National Institute for Materials Science, Tsukuba 305-0044, Japan*; orcid.org/0000-0003-3701-8119

Takashi Taniguchi − *International Center for Materials Nanoarchitectonics, National Institute for Materials Science, Tsukuba 305-0044, Japan*; orcid.org/0000-0002-1467-3105

Jing Wu − *Institute of Materials Research and Engineering, Agency for Science, Technology and Research, Singapore 138634, Singapore*

Kian Ping Loh − *Department of Chemistry, National University of Singapore, 117543, Singapore*; orcid.org/0000-0002-1491-743X

Michael F. Crommie − *Department of Physics, University of California, Berkeley 94720 California, United States*; orcid.org/0000-0001-8246-3444

Complete contact information is available at: https://pubs.acs.org/10.1021/acs.nanolett.2c02235

Author Contributions

M.T., A.R., and J.Lu. conceived the project. M.T. performed experiments related to ion implantation of Gr/BN, STM/STS measurements, and data analysis. K.N., H.B., D.D., Z.W.Y., and A.R. performed DFT and TB calculations. P.L., J.Li, and Z.C. fabricated a back-gated Gr/BN device under the guidance of K.P.L., J.W., H.-Z.T., and M.F.C.; K.W. and T.T. grew hBN crystals for the device. H.F. and Z.Q. assisted in STM experimental procedures. The manuscript was written by M.T., A.R., and J.Lu. with contributions from all coauthors.

Notes

The authors declare no competing financial interest.

■ ACKNOWLEDGMENTS

J. Lu acknowledges the support from MOE Tier 2 (MOE2019-T2-2-044 and MOE-T2EP50121-0008), MOE (Singapore) through the Research Centre of Excellence program (Grant No. EDUN C-33-18-279-V12, I-FIM), and Agency for Science, Technology and Research (A*STAR) under its AME IRG Grant (Project No. M21K2c0113). M. Telychko acknowledges the support from A*STAR AME YIRG grant (Project No. A20E6c0098, R-143-000-B71-305). A. Rodin acknowledges the National Research Foundation, Prime Minister Office, Singapore, under its Medium Sized Centre Programme and the support by Yale-NUS College (through Grant No. R-607-265-380-121). K.P. Loh acknowledges the funding support from MOE-T2EP50220-0002. K. Watanabe and T. Taniguchi acknowledge support from the Elemental Strategy Initiative conducted by the MEXT, Japan (Grant No. JPMXP0112101001) and JSPS KAKENHI (Grant Nos. 19H05790, 20H00354, and 21H05233). M.F.C. acknowledges support from the U.S. National Science Foundation under grant DMR-2221750.

■ REFERENCES

(1) Ni, G. X.; McLeod, A. S.; Sun, Z.; Wang, L.; Xiong, L.; Post, K. W.; Sunku, S. S.; Jiang, B. Y.; Hone, J.; Dean, C. R.; Fogler, M. M.; Basov, D. N. Fundamental limits to graphene plasmonics. *Nature* **2018**, *557*, 530−533.

(2) Fei, Z.; Rodin, A. S.; Andreev, G. O.; Bao, W.; McLeod, A. S.; Wagner, M.; Zhang, L. M.; Zhao, Z.; Thiemens, M.; Dominguez, G.; Fogler, M. M.; Castro Neto, A. H.; Lau, C. N.; Keilmann, F.; Basov, D. N. Gate-tuning of graphene plasmons revealed by infrared nano-imaging. *Nature* **2012**, *487*, 82−85.

(3) Wong, D.; Corsetti, F.; Wang, Y.; Brar, V. W.; Tsai, H. Z.; Wu, Q.; Kawakami, R. K.; Zettl, A.; Mostofi, A. A.; Lischner, J.; Crommie, M. F. Spatially resolving density-dependent screening around a single charged atom in graphene. *Phys. Rev. B* **2017**, *95*, 205419.

(4) Wang, Y.; Brar, V. W.; Shytov, A. V.; Wu, Q.; Regan, W.; Tsai, H.-Z.; Zettl, A.; Levitov, L. S.; Crommie, M. F. Mapping Dirac quasiparticles near a single Coulomb impurity on graphene. *Nat. Phys.* **2012**, *8*, 653−657.

(5) Wang, Y.; Brar, V. W.; Shytov, A. V.; Wu, Q.; Regan, W.; Tsai, H. Z.; Zettl, A.; Levitov, L. S.; Crommie, M. F. Mapping Dirac

quasiparticles near a single Coulomb impurity on graphene. *Nat. Phys.* **2012**, *8*, 653−657.
(6) Brar, V. W.; Decker, R.; Solowan, H. M.; Wang, Y.; Maserati, L.; Chan, K. T.; Lee, H.; Girit, Ç. O.; Zettl, A.; Louie, S. G.; Cohen, M. L.; Crommie, M. F. Gate-controlled ionization and screening of cobalt adatoms on a graphene surface. *Nat. Phys.* **2011**, *7*, 43−47.
(7) Wang, Y.; Wong, D.; Shytov, A. V.; Brar, V. W.; Choi, S.; Wu, Q.; Tsai, H.-Z.; Regan, W.; Zettl, A.; Kawakami, R. K.; Louie, S. G.; Levitov, L. S.; Crommie, M. F. Observing Atomic Collapse Resonances in Artificial Nuclei on Graphene. *Science* **2013**, *340*, 734−737.
(8) Tsai, H.-Z.; et al. A molecular shift register made using tunable charge patterns in one-dimensional molecular arrays on graphene. *Nature Electronics* **2020**, *3*, 598−603.
(9) Lu, J.; Tsai, H. Z.; Tatan, A. N.; Wickenburg, S.; Omrani, A. A.; Wong, D.; Riss, A.; Piatti, E.; Watanabe, K.; Taniguchi, T.; Zettl, A.; Pereira, V. M.; Crommie, M. F. Frustrated supercritical collapse in tunable charge arrays on graphene. *Nature Commun.* **2019**, *10*, 1−8.
(10) Mao, J.; Jiang, Y.; Moldovan, D.; Li, G.; Watanabe, K.; Taniguchi, T.; Masir, M. R.; Peeters, F. M.; Andrei, E. Y. Realization of a tunable artificial atom at a supercritically charged vacancy in graphene. *Nat. Phys.* **2016**, *12*, 545−549.
(11) Pereira, V. M.; Nilsson, J.; Castro Neto, A. H. Coulomb impurity problem in graphene. *Phys. Rev. Lett.* **2007**, *99*, 166802.
(12) Shytov, A. V.; Katsnelson, M. I.; Levitov, L. S. Atomic collapse and quasi-rydberg states in graphene. *Phys. Rev. Lett.* **2007**, *99*, 246802.
(13) Shytov, A. V.; Katsnelson, M. I.; Levitov, L. S. Vacuum polarization and screening of supercritical impurities in graphene. *Phys. Rev. Lett.* **2007**, *99*, 236801.
(14) Zhang, Y.; Gao, F.; Gao, S.; He, L. Tunable magnetism of a single-carbon vacancy in graphene. *Science Bulletin* **2020**, *65*, 194−200.
(15) Telychko, M.; Mutombo, P.; Ondráček, M.; Hapala, P.; Bocquet, F. C.; Kolorenč, J.; Vondráček, M.; Jelínek, P.; Švec, M. Achieving high-quality single-atom nitrogen doping of graphene/SiC(0001) by ion implantation and subsequent thermal stabilization. *ACS Nano* **2014**, *8*, 7318−7324.
(16) Telychko, M.; Mutombo, P.; Merino, P.; Hapala, P.; Ondráček, M.; Bocquet, F. C.; Sforzini, J.; Stetsovych, O.; Vondráček, M.; Jelínek, P.; Švec, M. Electronic and Chemical Properties of Donor, Acceptor Centers in Graphene. *ACS Nano* **2015**, *9*, 9180−9187.
(17) Lagoute, J.; Joucken, F.; Repain, V.; Tison, Y.; Chacon, C.; Bellec, A.; Girard, Y.; Sporken, R.; Conrad, E. H.; Ducastelle, F.; Palsgaard, M.; Andersen, N. P.; Brandbyge, M.; Rousset, S. Giant tunnel-electron injection in nitrogen-doped graphene. *Phys. Rev. B* **2015**, *91*, 125442.
(18) González-Herrero, H.; Gómez-Rodríguez, J. M.; Mallet, P.; Moaied, M.; Palacios, J. J.; Salgado, C.; Ugeda, M. M.; Veuillen, J. Y.; Yndurain, F.; Brihuega, I. Atomic-scale control of graphene magnetism by using hydrogen atoms. *Science* **2016**, *352*, 437−441.
(19) Mallada, B.; Edalatmanesh, S.; Lazar, P.; Redondo, J.; Gallardo, A.; Zbořil, R.; Jelínek, P.; Švec, M.; De La Torre, B. Atomic-Scale Charge Distribution Mapping of Single Substitutional p- And n-Type Dopants in Graphene. *ACS Sustainable Chem. Eng.* **2020**, *8*, 3437−3444.
(20) Zhao, L.; et al. Visualizing Individual Nitrogen Dopants in Monolayer Graphene. *Science* **2011**, *333*, 999−1004.
(21) Wang, H.; Maiyalagan, T.; Wang, X. Review on recent progress in nitrogen-doped graphene: Synthesis, characterization, and its potential applications. *ACS Catal.* **2012**, *2*, 781−794.
(22) Joucken, F.; Henrard, L.; Lagoute, J. Electronic properties of chemically doped graphene. *Phys. Rev. Mater.* **2019**, *3*, 110301.
(23) Van Der Heijden, N. J.; Smith, D.; Calogero, G.; Koster, R. S.; Vanmaekelbergh, D.; Van Huis, M. A.; Swart, I. Recognizing nitrogen dopant atoms in graphene using atomic force microscopy. *Phys. Rev. B* **2016**, *93*, 245430.
(24) Joucken, F.; Bena, C.; Ge, Z.; Quezada-Lopez, E. A.; Ducastelle, F. m. c.; Tanagushi, T.; Watanabe, K.; Velasco, J. Sublattice Dependence and Gate Tunability of Midgap and Resonant States Induced by Native Dopants in Bernal-Stacked Bilayer Graphene. *Phys. Rev. Lett.* **2021**, *127*, 106401.
(25) Sforzini, J.; Hapala, P.; Franke, M.; Van Straaten, G.; Stöhr, A.; Link, S.; Soubatch, S.; Jelínek, P.; Lee, T. L.; Starke, U.; Švec, M.; Bocquet, F. C.; Tautz, F. S. Structural and Electronic Properties of Nitrogen-Doped Graphene. *Phys. Rev. Lett.* **2016**, *116*, 126805.
(26) Tripathi, M.; Mittelberger, A.; Pike, N. A.; Mangler, C.; Meyer, J. C.; Verstraete, M. J.; Kotakoski, J.; Susi, T. Electron-Beam Manipulation of Silicon Dopants in Graphene. *Nano Lett.* **2018**, *18*, 5319−5323.
(27) de la Torre, B.; Švec, M.; Hapala, P.; Redondo, J.; Krejčí, O.; Lo, R.; Manna, D.; Sarmah, A.; Nachtigallová, D.; Tuček, J.; Błoński, P.; Otyepka, M.; Zbořil, R.; Hobza, P.; Jelínek, P. Non-covalent control of spin-state in metal-organic complex by positioning on N-doped graphene. *Nature C* **2018**, *9*, 1−9.
(28) Lin, L.; et al. Nitrogen cluster doping for high-mobility/conductivity graphene films with millimeter-sized domains. *Sci. Adv.* **2019**, *5*, No. eaaw8337.
(29) Bouatou, M.; Mondal, S.; Chacon, C.; Joucken, F.; Girard, Y.; Repain, V.; Bellec, A.; Rousset, S.; Narasimhan, S.; Sporken, R.; Dappe, Y. J.; Lagoute, J. Direct Observation of the Reduction of a Molecule on Nitrogen Pairs in Doped Graphene. *Nano Lett.* **2020**, *20*, 6908−6913.
(30) Joucken, F.; Tison, Y.; Lagoute, J.; Dumont, J.; Cabosart, D.; Zheng, B.; Repain, V.; Chacon, C.; Girard, Y.; Botello-Méndez, A. R.; Rousset, S.; Sporken, R.; Charlier, J.-C.; Henrard, L. Localized state and charge transfer in nitrogen-doped graphene. *Phys. Rev. B* **2012**, *85*, 161408.
(31) Dean, C. R.; Young, A. F.; Meric, I.; Lee, C.; Wang, L.; Sorgenfrei, S.; Watanabe, K.; Taniguchi, T.; Kim, P.; Shepard, K. L.; Hone, J. Boron nitride substrates for high-quality graphene electronics. *Nature Nanotechnol* **2010**, *5*, 722−726.
(32) Dutreix, C.; González-Herrero, H.; Brihuega, I.; Katsnelson, M. I.; Chapelier, C.; Renard, V. T. Measuring the Berry phase of graphene from wavefront dislocations in Friedel oscillations. *Nature* **2019**, *574*, 219−222.
(33) Ugeda, M. M.; Brihuega, I.; Guinea, F.; Gómez-Rodríguez, J. M. Missing atom as a source of carbon magnetism. *Phys. Rev. Lett.* **2010**, *104*, 096804.
(34) Zhang, Y.; Brar, V. W.; Wang, F.; Girit, C.; Yayon, Y.; Panlasigui, M.; Zettl, A.; Crommie, M. F. Giant phonon-induced conductance in scanning tunnelling spectroscopy of gate-tunable graphene. *Nat. Phys.* **2008**, *4*, 627−630.
(35) Wong, D.; Velasco, J.; Ju, L.; Lee, J.; Kahn, S.; Tsai, H. Z.; Germany, C.; Taniguchi, T.; Watanabe, K.; Zettl, A.; Wang, F.; Crommie, M. F. Characterization and manipulation of individual defects in insulating hexagonal boron nitride using scanning tunnelling microscopy. *Nature Nanotechnol* **2015**, *10*, 949−953.
(36) Qiu, Z.; et al. Giant gate-tunable bandgap renormalization and excitonic effects in a 2D semiconductor. *Science Advances* **2019**, *5*, No. eaaw2347.
(37) Decker, R.; Wang, Y.; Brar, V. W.; Regan, W.; Tsai, H.-Z.; Wu, Q.; Gannett, W.; Zettl, A.; Crommie, M. F. Local Electronic Properties of Graphene on a BN Substrate via Scanning Tunneling Microscopy. *Nano Lett.* **2011**, *11*, 2291−2295. PMID: 21553853.
(38) Noori, K.; Biswas, H.; Quek, S. Y.; Rodin, A. Graphene-mediated interaction between hydrogen adsorbates. *Phys. Rev. B* **2020**, *101*, 115421.
(39) Wickenburg, S.; et al. Tuning charge and correlation effects for a single molecule on a graphene device. *Nature Commun.* **2016**, *7*, 1−7.
(40) Lambin, P.; Amara, H.; Ducastelle, F.; Henrard, L. Long-range interactions between substitutional nitrogen dopants in graphene: Electronic properties calculations. *Physical Review B - Condensed Matter and Materials Physics* **2012**, *86*, 045448.
(41) Noori, K.; Quek, S. Y.; Rodin, A. Hydrogen adatoms on graphene: The role of hybridization and lattice distortion. *Phys. Rev. B* **2020**, *102*, 195416.

https://doi.org/10.1021/acs.nanolett.2c02235
Nano Lett. 2022, 22, 8422−8429

(42) Bezanson, J.; Edelman, A.; Karpinski, S.; Shah, V. B. Julia: A Fresh Approach to Numerical Computing. *arXiv* **2017**, DOI: 10.48550/arXiv.1411.1607.
(43) Rodin, A.; Mahalingam, H.*GrapheneQFT. 2021*; https://github.com/rodin-physics/GrapheneQFT.jl, accessed 2022-03-10.
(44) Joucken, F.; Bena, C.; Ge, Z.; Quezada-Lopez, E.; Pinon, S.; Kaladzhyan, V.; Taniguchi, T.; Watanabe, K.; Ferreira, A.; Velasco, J. Direct Visualization of Native Defects in Graphite and Their Effect on the Electronic Properties of Bernal-Stacked Bilayer Graphene. *Nano Lett.* **2021**, *21*, 7100−7108. PMID: 34415771.
(45) Wang, G.; et al. Seamless lateral graphene p−n junctions formed by selective in situ doping for high-performance photodetectors. *Nat. Commun.* **2018**, *9*, 5168.
(46) Lin, L.; Liao, L.; Yin, J.; Peng, H.; Liu, Z. Building graphene p−n junctions for next-generation photodetection. *Nano Today* **2015**, *10*, 701−716.
(47) Lee, J.; Wong, D.; Velasco, J.; Rodriguez-Nieva, J. F.; Kahn, S.; Tsai, H. Z.; Taniguchi, T.; Watanabe, K.; Zettl, A.; Wang, F.; Levitov, L. S.; Crommie, M. F. Imaging electrostatically confined Dirac fermions in graphene quantum dots. *Nat. Phys.* **2016**, *12*, 1032−1036.
(48) Ge, Z.; Joucken, F.; Quezada, E.; da Costa, D. R.; Davenport, J.; Giraldo, B.; Taniguchi, T.; Watanabe, K.; Kobayashi, N. P.; Low, T.; Velasco, J. Visualization and Manipulation of Bilayer Graphene Quantum Dots with Broken Rotational Symmetry and Nontrivial Topology. *Nano Lett.* **2020**, *20*, 8682−8688.
(49) Ge, Z.; Wong, D.; Lee, J.; Joucken, F.; Quezada-Lopez, E. A.; Kahn, S.; Tsai, H.-Z.; Taniguchi, T.; Watanabe, K.; Wang, F.; Zettl, A.; Crommie, M. F.; Velasco, J. Imaging Quantum Interference in Stadium-Shaped Monolayer and Bilayer Graphene Quantum Dots. *Nano Lett.* **2021**, *21*, 8993−8998.
(50) Hwang, E. H.; Das Sarma, S. Impurity-scattering-induced carrier transport in twisted bilayer graphene. *Phys. Rev. Research* **2020**, *2*, 013342.

NOTE ADDED AFTER ASAP PUBLICATION

This paper was published ASAP on October 10, 2022 with a typo in the caption of Figure S7 in the Supporting Information file. The corrected version was reposted on October 19, 2022.

https://doi.org/10.1021/acs.nanolett.2c02235
Nano Lett. 2022, 22, 8422−8429